Comprehensive stratum corneum ceramide profiling reveals reduced acylceramides in ichthyosis patient with *CERS3* mutations

Moe Yamamoto,[1] Takayuki Sassa,[1] Yuki Kyono,[2] Hiroyasu Uemura,[3] Masaaki Kugo,[3] Hideki Hayashi,[4] Yasutomo Imai,[4] Kiyofumi Yamanishi,[4,*] and Akio Kihara[1,*]

[1]*Laboratory of Biochemistry, Faculty of Pharmaceutical Sciences, Hokkaido University, Sapporo, Japan*

[2]*Department of Pediatrics, Kobe University Graduate School of Medicine, Kobe, Japan*

[3]*Department of Pediatrics, Japanese Red Cross Society Himeji Hospital, Himeji, Japan*

[4]*Department of Dermatology, Hyogo College of Medicine, Nishinomiya, Japan*

[*]To whom correspondence should be addressed:

Kiyofumi Yamanishi

Department of Dermatology

Hyogo College of Medicine

1-1 Mukogawa-cho, Nishinomiya, Hyogo 663-8501, Japan

E-mail: kyamanis@hyo-med.ac.jp

Akio Kihara

Laboratory of Biochemistry, Faculty of Pharmaceutical Sciences

Hokkaido University

Kita 12-jo, Nishi 6-chome, Kita-ku, Sapporo 060-0812, Japan

E-mail: kihara@pharm.hokudai.ac.jp

Running title: *CERS3* mutations reduce acylceramides

Abbreviations: A, α-hydroxy fatty acid; acylceramides, ω-*O*-acylceramides; ARCI, autosomal recessive congenital ichthyosis; CERS, ceramide synthase; CLE, corneocyte lipid envelope; d_7, seven deuterium; DS, dihydrosphingosine; EO, esterified ω-hydroxy fatty acid; FA, fatty acid; H, 6-hydroxy sphingosine; LCB, long-chain base; LC–MS/MS, liquid chromatography–tandem mass spectrometry; N, non-hydroxy fatty acid; O, ω-hydroxy fatty acid; P, phytosphingosine; P-O, protein-bound ω-hydroxy fatty acid; S, sphingosine; SC, stratum corneum; SD, 4,14-sphingadiene; WT, wild-type.

ABSTRACT

The stratum corneum (SC) of the epidermis acts as a skin permeability barrier, and abnormalities in SC formation lead to several skin disorders. Lipids, especially the epidermis-specific ceramide classes ω-*O*-acylceramides (acylceramides) and protein-bound ceramides, are essential for skin barrier formation. Ceramide synthase 3 (CERS3) is involved in the synthesis of acylceramides and protein-bound ceramides, and *CERS3* mutations cause autosomal recessive congenital ichthyosis. In the present study, we measured CERS activity and performed comprehensive SC ceramide profiling in an ichthyosis patient with compound heterozygous *CERS3* mutations: nonsense mutation p.Arg75* and missense mutation p.Arg229His. The activity of p.Arg75* and p.Arg229His mutant CERS3 proteins was reduced to 4% and 56%, respectively, of the wild-type protein. In the patient's SC, acylceramide levels were greatly reduced, but the levels of protein-bound ceramides remained almost unchanged. Non-acylated ceramide levels were also affected in the patient; in particular, the levels of ceramides composed of sphingosine and non-hydroxy or α-hydroxy fatty acid were substantially higher than in healthy controls. These results suggest that a reduction in acylceramide levels alone leads to ichthyosis. Although protein-bound ceramides are synthesized from acylceramides, levels of acylceramides and protein-bound ceramides are not necessarily correlated.

KEYWORDS: acylceramide, ceramide, ichthyosis, sphingolipid, stratum corneum

INTRODUCTION

The skin permeability barrier is important for protection from the invasion of microorganisms, external chemicals, and allergens and the prevention of transepidermal water loss. A functional defect in this barrier leads to skin disorders such as infections, allergic dermatitis, and ichthyosis.[1-3] The epidermis comprises four layers, in order from the outside to the inside: stratum corneum (SC), stratum granulosum, stratum spinosum, and stratum basale. Of these, the SC is the most crucial for the skin's permeability barrier function. The SC is composed of corneocytes, which are enucleated dead keratinocytes, and lipid lamellae that fill the extracellular spaces between the corneocytes. The lipid lamella is a multilayered structure composed mainly of ceramides, fatty acids (FAs), and cholesterol.[4] These lamellar ceramides belong to various classes, including the epidermis-specific acylceramides (ω-*O*-acylceramides).[5,6] The surface of corneocytes is covered by the corneocyte lipid envelope (CLE), which consists of protein-bound ceramides that are covalently bound to the cornified envelope.[7,8] Mutations in genes related to the synthesis of ceramides, acylceramides, and protein-bound ceramides cause autosomal recessive congenital ichthyosis (ARCI), which is a severe form of ichthyosis.[2,3] ARCI is further classified into harlequin ichthyosis, lamellar ichthyosis, and congenital ichthyosiform erythroderma.[2,3]

Ceramides form the hydrophobic backbone of sphingolipids and typically consist of two hydrophobic chains: a long-chain base (LCB) and an FA (Fig. 1a).[6] However, acylceramides are unusual in that they have an additional hydrophobic chain, linoleic acid, which is esterified to the ω-hydroxy group of the FA in the ceramide backbone. This unique structure is necessary for the formation and maintenance of the lipid lamellae. Human ceramides consist of one of the five types of LCB, which differ in the number and position of the double bond and hydroxyl

group: dihydrosphingosine, sphingosine, phytosphingosine, 6-hydroxy sphingosine, and 4,14-sphingadiene (Fig. 1b).[6,9] In addition, one of the three FA types (non-hydroxy, α-hydroxy, and ω-hydroxy) are present in human ceramides; these differ in the number and position of the hydroxyl group (Fig. 1c). In the human SC, most ω-hydroxy ceramides are esterified with linoleic acid, forming acylceramides. Based on the combinations of LCBs and FAs (including esterified ones), human ceramides are categorized into 20 classes. Each ceramide class is represented using a combination of the abbreviation of the FA type (N, non-hydroxy; A, α-hydroxy; O, ω-hydroxy; EO, esterified ω-hydroxy) and the LCB type (DS, dihydrosphingosine; S, sphingosine; P, phytosphingosine; H, 6-hydroxy sphingosine; SD, 4,14-sphingadiene) (Fig. 1d). Thus, EOS, EODS, EOH, EOP, and EOSD are acylceramides. Some acylceramides are metabolized into protein-bound ceramides comprising one of the five LCBs and a protein-bound ω-hydroxy (P-O) FA.[8,10]

Ceramide synthase (CERS) is involved in the synthesis of ceramides from an LCB and an acyl-CoA. Mammals have six CERS isozymes (CERS1–6) exhibiting distinct substrate specificities toward acyl-CoAs with different chain lengths.[6] CERS3 utilizes mainly acyl-CoAs with a chain length of ≥ C26 as substrates and catalyzes the synthesis of acylceramides and protein-bound ceramides containing C28–C36 FAs (Fig. 1a).[11] *CERS3* is one of the ARCI-causative genes (OMIM number, 615023).[12,13] *Cers3* knockout mice exhibit reduced epidermal levels of acylceramides, protein-bound ceramides, and non-acylated ceramides containing ≥ C26 FAs, which in turn led to severe impairment of skin permeability barrier formation and neonatal lethality.[11]

So far, 11 distinct *CERS3* mutations have been identified in ARCI patients.[12-16] However, CERS3 activity has been measured for only one mutation (p.Trp15Arg), and ceramide

quantification has been performed for only two mutations (p.Trp15Arg and a splice donor mutation) and on limited ceramide classes: four (NS, OS, EOS, and P-OS) for the p.Trp15Arg mutation and three (NS, NP, and EOS) for the splice donor mutation.[12,13] Thus, the effect of the mutations on SC ceramide composition is not completely understood. In addition, because these studies were conducted using cultured patient-derived keratinocytes, their results may not accurately reflect the changes in SC ceramide levels and composition in the patients. Although levels of both acylceramides and protein-bound ceramides are diminished due to complete loss of CERS3 activity in *Cers3* knockout mice,[11] most actual human mutations are missense mutations that may cause residual CERS3 activity. Therefore, clarifying how ceramide composition changes and how it is linked to the pathology in actual patients is necessary.

Here, we studied an ARCI patient with compound heterozygous *CERS3* mutations [a nonsense mutation (p.Arg75*) and a missense mutation (p.Arg229His)]. In addition to measuring the enzyme activity of the mutant proteins, we comprehensively analyzed the SC ceramides in the patient using our recently established liquid chromatography–tandem mass spectrometry (LC–MS/MS) method.[9]

METHODS

Ethics

This study was approved by the Ethics Review Board for Human Genome/Gene Analysis Research, Hyogo College of Medicine (Permit Number: 32) and by the ethics committee of Hokkaido University (Permit Number: 2019-001-2). Informed consent was obtained from all participants in the study, and the research was conducted according to the principles expressed in the Declaration of Helsinki.

Whole exome sequencing of genomic DNA

Whole exome sequencing was outsourced to BGI Japan (Kobe, Japan). An exome library from the patient's genomic DNA was prepared using the SureSelect Human All Exon V6 kit (Agilent Technologies, Santa Clara, CA, USA), and sequence reads were obtained using the HiSeq2500 system (Illumina, San Diego, CA, USA). The reads were provided as Fastq files from BGI Japan and were aligned to the human genome assembly hg19. The average read depth was 50, and 89.56% of the targeted bases were covered by more than 20 reads. Nucleotide variants were identified using SureCall v.3 (Agilent Technologies) and Reseq (Amelieff, Tokyo, Japan).

Sanger sequencing of *CERS3* genomic DNA

Sanger sequencing of the PCR products from the patient and his parents, spanning nucleotides 53915–54522 and 71610–72471 of the *CERS3* genomic DNA sequence NC_000015.10 (100400395..100544982, complement), was performed using a BigDye Terminator v3.1 Cycle Sequencing Kit (Thermo Fisher Scientific, Waltham, MA, USA). For c.223C>T, PCR primers 5′-GGCTGTACGTAGCCCCAGTG-3′ and 5′-GGGCTTCTCTGCCCTAACAATTA-3′ and

sequencing primer 5′-GTTACAGCTTTAATTTTCTGGTGTCA-3′ were used; for c.686G>A, PCR primers 5′-AGGCAGGGGCTAAACAATAAC-3′ and 5′-GGGAGTGTGAACATTCAACGG-3′ and sequencing primer 5′-TCTTCCAGTGATTGGGAAAT-3′ were used. The sequences obtained were analyzed using the Applied Biosystems 3130xL or 3500xL Genetic Analyzer (Thermo Fisher Scientific).

Plasmids

Mammalian expression vectors pEFh-3×FLAG-1[17] and pCE-puro-3×FLAG-1,[18] designed to express N-terminal 3×FLAG-tagged proteins, were used for expressing CERS3 and ELOVL1 proteins. The pCE-puro-3×FLAG-ELOVL1 plasmid was described previously.[19] The pEFh-3×FLAG-CERS3 plasmid was constructed by transferring *CERS3* from pCE-puro-3×FLAG-CERS3[20] to the pEFh-3×FLAG-1 vector. The p.Arg75*- and p.Arg229His-encoding *CERS3* mutant cDNAs were generated via PCR and overlap extension PCR, respectively, using *CERS3* WT cDNA and primers (p.Arg75*, 5′-GGATCCATGTTTTGGACGTTTAAAGAATGG-3′ and 5′-TTCAAACTGTCTCTTTAATGCCAAATGATTTTGC-3′; p.Arg229His, 5′-GGATCCATGTTTTGGACGTTTAAAGAATGG-3′, 5′-GCTAATTATATTCACAGTGGGACCCTCGTGATGATTGTACACG-3′, 5′-CCCACTGTGAATATAATTAGCACACCAAGAGAAGC-3′, and 5′-CTAATGGCCATGCTGGCCATTGGG-3′). This was followed by cloning into the pEFh-3×FLAG-1 vector to produce pEFh-3×FLAG-CERS3 (p.Arg75*) and pEFh-3×FLAG-CERS3 (p.Arg229His) plasmids.

Cell culture and transfection

HEK 293T cells were seeded in 0.3% collagen-coated dishes (Nitta Gelatin, Osaka, Japan) and cultured in Dulbecco's modified Eagle's medium (Merck, Darmstadt, Germany) in a humidified atmosphere of 5% CO_2 at 37 °C; the medium was supplemented with 10% fetal bovine serum, 100 units/ml penicillin, and 100 µg/ml streptomycin. The cells were transfected using the reagents Lipofectamine and PLUS (Thermo Fisher Scientific), according to the manufacturer's instructions.

CERS assay

HEK 293T cells were transfected with the pCE-puro-3×FLAG-ELOVL1 plasmid together with the pEFh-3×FLAG-1, pEFh-3×FLAG-CERS3, pEFh-3×FLAG-CERS3 (p.Arg229His) or pEFh-3×FLAG-CERS3 (p.Arg75*) plasmid. At 24 h after transfection, the cells were treated with 5 µM seven deuterium (d_7) atom-containing DS (Avanti Polar Lipids, Alabaster, AL, USA) at 37 °C for 3 h. After the cells had been washed with phosphate-buffered saline, they were collected using a scraper and centrifuged (800 × *g*, room temperature, 3 min). Subsequently, lipid extraction was performed as follows. The cells were resuspended in 100 µl of water and mixed with 375 µl of chloroform/methanol (1:2, v/v) containing 1.5 pmol of d_9-C16:0 NS (Avanti Polar Lipids) for use as an internal standard for LC–MS/MS analysis. The mixture was then subjected to alkaline hydrolysis of ester bond-containing lipids by adding 12.5 µl of 3 M potassium hydroxide in methanol and incubating the mixture at 37 °C for 1 h. After the mixture was neutralized by adding 13 µl of 3 M formic acid in water, phases were separated by adding 125 µl of chloroform and 125 µl of water and by subsequent centrifugation (20,400 × *g*, room temperature, 3 min). The organic phase was recovered and dried. Lipids were dissolved in chloroform/methanol (1:2, v/v), and d_7-C26:0 NS ceramide was analyzed using

LC–MS/MS as described previously,[9,20] using the following settings in multiple reaction monitoring mode: precursor ion (Q1, $[M-H_2O + H]^+$), m/z = 667.7; product ion (Q3), m/z = 271.3; collision energy, 30 eV. CERS3 activity was calculated as the difference in the quantity of d_7-C26:0 NS ceramide between the cells with *CERS3* plasmid transfection and the control cells without transfection.

Immunoblotting

As described previously,[21] immunoblotting was performed using rabbit anti-FLAG polyclonal antibody (1:1,000 dilution) and anti-rabbit IgG, HRP-linked $F(ab')_2$ fragment (1:7,500 dilution; GE Healthcare Life Sciences, Little Chalfont, UK) as primary and secondary antibodies, respectively. Chemiluminescence was produced using Pierce ECL Western Blotting Substrate (Thermo Fischer Scientific).

Preparation and quantification of SC ceramides

SC samples from the skin of the back were collected from the male ichthyosis patient (age: 1 year) and three healthy male individuals (ages: 1, 2, and 31 years), as described previously.[9] From each tape strip, three 10 × 10 mm pieces were cut, which were used as replicates of that sample. The extraction of lipids from tape strips, preparation of free and protein-bound ceramides, and LC–MS/MS quantification of these species as well as the internal standard lipids used were done as described previously.[9] Briefly, methanol (800 μl) was added to the tape to extract the lipids. After the tape was removed, the samples were centrifuged. The supernatant was dried and subjected to LC–MS/MS analysis to measure the free ceramides. The pellet was suspended in 800 μl of methanol and then divided in two; one half was used for protein

quantification and the other for the measurement of protein-bound ceramides via LC–MS/MS. For protein quantification, samples were dried, suspended in 45 μl of 0.1 M NaOH and 1% SDS, and dissolved by incubating them for 2 h at 60 °C, with vigorous mixing every 30 min. After the addition of 5 μl of 1 M HCl and 0.5 M Tris HCl (pH 6.8) to the samples for neutralization, protein quantities were measured using a Pierce BCA Protein Assay Kit (Thermo Fisher Scientific). The lipid levels determined in the LC–MS/MS analysis were normalized by these protein quantities.

RESULTS

ARCI patient harboring compound heterozygous *CERS3* mutations

The patient was a Japanese boy born at the gestational age of 35 weeks and 1 day with a birth weight of 1,744 g. At birth, he had taut, erythrodermic skin with mild ectropion, eclabium, and bilateral auricular hypoplasia. He also had bilateral cryptorchidism, but no other malformations were observed. He showed no signs of respiratory disorders or infections. However, to avoid hypothermia, he was kept at optimal temperature and humidity in an incubator, and ampicillin was administered prophylactically. From postnatal day 3, his exfoliation of scales and erythema increased, and azulene ointment was topically applied. Around postnatal day 10, his body temperature stabilized, and bathing was initiated. The patient was his parents' first child, and the family had no history of ARCI. Because there was no progressive exacerbation of his cutaneous conditions, he was treated only with topical white petrolatum. At two months of age, he had erythroderma with fine scale and wrinkles, limited desquamation (Fig. 2a), and mild palmoplantar keratoderma. The ectropion and eclabium had improved, and there was no evident alopecia, nail dystrophy, or acrogeria of the hands or feet. Congenital ichthyosiform erythroderma was diagnosed based on the patient's clinical findings and course.

Whole-exome sequencing of the patient's genomic DNA revealed compound heterozygous single-nucleotide variants within *CERS3*, which is located on chromosome 15: c.223C>T (nonsense mutation p.Arg75*) and c.686G>A (missense mutation p.Arg229His), corresponding respectively to g.101031087G>A (−) in exon 5 and g.101013181C>T (−) in exon 10 of *CERS3* in the DNA sequence with Ref. ID NM_001290342.2 (Fig. 2b and Supplementary Fig. S1a, b). The patient's father and mother were heterozygous carriers of the mutations c.223C>T (p.Arg75*) and c.686G>A (p.Arg229His), respectively (Fig. 2b). The

c.223C>T (p.Arg75*) mutation is listed in the Genome Aggregation Database v.2.1.1 (https://gnomad.broadinstitute.org) but has not been reported in patients with ARCI. The c.686G>A (p.Arg229His) mutation has been reported in a family with ARCI in Iran.[15] The Arg75 residue is located in the cytosolic loop between transmembrane regions 1 and 2 in the CERS membrane topology model (Fig. 2c).[22] The Arg229 residue is located in the next cytosolic loop, which constitutes the Lag1 motif. This is a highly conserved motif in CERS family proteins and contains several residues essential for CERS catalytic activity.[23]

Decreased CERS3 activity due to ichthyosis mutations

We measured the activity of the p.Arg75* and p.Arg229His mutant proteins. For this measurement, 3×FLAG-tagged CERS3 wild-type (WT) or mutant protein was co-expressed with 3×FLAG-ELOVL1 in HEK 293T cells. ELOVL1 is an FA elongase that produces C26:0-CoA, the CERS3 substrate.[11,19,24,25] The cells were labeled with d_7-DS, and d_7-labeled NS ceramides were quantified using LC–MS/MS. CERS3 WT protein expression increased d_7-C26:0 NS ceramide levels 3.5-fold relative to the control (Fig. 3a). Levels of d_7-C26:0 NS ceramide produced by the CERS3 mutant proteins were significantly lower than those produced by the WT protein (p.Arg229His: 56% of the WT protein; p.Arg75*: 4%). The amount of NS ceramide produced in cells expressing the p.Arg75* mutant protein was comparable to that in the vector-transfected cells. ELOVL1 and CERS3 were expressed at similar levels in all the cells (Fig. 3b). These results show that the p.Arg75* mutation completely abolishes CERS3 activity, whereas the p.Arg229His mutation leads only to reduced CERS3 activity.

Reduced acylceramide levels in the patient's SC

To examine the effect of *CERS3* mutations on the SC ceramide profile, we comprehensively analyzed the ceramides in SC samples using LC–MS/MS. The samples were taken from the patient and three healthy individuals who served as controls. Consistent with the results of our previous report,[9] the control SC was rich in three ceramide classes: NP, NH, and AH (24.0%, 22.2%, and 17.2% of total ceramides, respectively) (Fig. 4a,b, Supplementary Table S1). The eight next most abundant classes were, in descending order, AP, NDS, AS, EOH, NS, EOS, EOP, and ADS (1.1–7.6%). The remaining nine classes each constituted less than 1% of total ceramides, and OSD was undetectable. Ceramide class composition in the patient and control SC were clearly different. Most notably, all five classes of acylceramides (EOH, EOS, EOP, EODS, and EOSD) were only present in small quantities in the patient's SC. NP, NH, and AH were present in lower quantities in the patient's SC than in the control SC, but AS, NS, NDS, AP, ADS, and OS were more abundant. The proportions of AS and NS were the highest (21.1% and 20.5%, respectively). Considering the ceramide classes categorized according to their LCB moiety, H- and P-type ceramides were abundant in the control SC (44.1% and 32.7%, respectively; Fig. 4c, Supplementary Table S1) and less so in the patient's SC (24.6% and 17.3%, respectively), whereas the proportions of S- and DS-type ceramides were higher (43.5% and 14.3%, respectively). When the ceramide classes are categorized according to their FA moiety, the proportion of N-type ceramides was the highest in both control and patient (control, 55.8%; patient, 49.7%; Fig. 4d, Supplementary Table S1). The proportion of EO-type ceramides (acylceramides) was considerably lower in the patient's SC than in the control SC (1.3% versus 11.6%), as described above, while that of A-type ceramides was higher (46.5% versus 31.2%). The ceramide composition of the SC was thus greatly affected by the *CERS3* mutations.

Each ceramide class consists of many species that differ in FA chain length. We compared the FA composition of 20 ceramide classes between the patient and control SC (Supplementary Table S2), and we present that of NS, AS, and EOS as representative examples (Fig. 4e–g). The predominant NS FA chain lengths in the control SC were C26:0, C24:0, C28:0, C25:0, and C16:0, in descending order of abundance (Fig. 4e). In the patient's SC, the predominant NS FA chain lengths were C18:0, C24:0, C16:0, C22:0, and C28:0, in descending order, and levels of all NS species except C26:0 NS were higher than in the control SC. Overall, the weighted-average FA chain length was shorter in the patient's SC (C21.8) than in the control (C24.4). In the AS class, the top three species in the control SC were C26:0, C16:0, and C24:0, whereas in the patient's SC, C16:0 was by far the most abundant species (Fig. 4f). The C14–C24 AS species were more abundant in the patient than the control SC, but the ≥ C25 AS species were less so. Again, the weighted-average FA chain length was shorter in the patient's SC (C18.1) than in the control SC (C22.6). In the EOS class, the C30:0 species was the most abundant in the control SC, followed by C32:0, C28:0, C31:0, C29:0, C34:1, and C32:1 (Fig. 4g). In the patient's SC, all EOS species were present in much lower quantities, regardless of FA chain length. Again, the tendency was for shorter FAs to be more common, and the C28:0 species was the most abundant. In summary, the FA chain lengths of all ceramide classes were shorter in the patient's SC than the control SC.

Normal quantities of protein-bound ceramides in the patient's SC

We also conducted LC–MS/MS analyses to examine the effect of *CERS3* mutations on protein-bound ceramide levels. In the control SC, P-OS was the most abundant species, followed by P-OH (Fig. 5a, Supplementary Table S3), which was consistent with the results of previous

reports.[9,26] The patient's SC contained almost the same quantities of P-OS and P-OH as the control SC. The FA composition of all the protein-bound ceramides, as illustrated for P-OS in Fig. 5b, differed little between the control and patient's SC (Supplementary Table S4). Thus, the patient's SC exhibited a unique ceramide profile: low acylceramide levels but normal levels of protein-bound ceramides.

DISCUSSION

Until now, the role of acylceramides and protein-bound ceramides in skin permeability barrier formation has been investigated mainly by analyzing mouse models deficient in the genes involved in their synthesis. Disruption of acylceramide synthesis-related genes (*Cers3*, *Cyp4f39*, and *Pnpla1*) reduces not only acylceramide levels but also protein-bound ceramide levels, because acylceramides are precursors of protein-bound ceramides.[11,27-29] By contrast, in mice deficient in genes (*Alox12b*, *Aloxe3*, and *Sdr9c7*) involved in the conversion of acylceramides to protein-bound ceramides, only protein-bound ceramide synthesis is impaired, and acylceramide levels remain largely unaffected.[10,30,31] All these mice exhibited severe abnormalities in skin permeability barrier formation and total neonatal lethality. These analyses revealed the importance of protein-bound ceramides in skin permeability barrier formation. However, they have not elucidated the contribution of acylceramides alone to skin permeability barrier formation, because of the lack of model mice deficient only in acylceramides.

In mice deficient in the genes involved in the synthesis of acylceramides and protein-bound ceramides, the respective genes are nullified (knocked out completely), and their functions are completely lost. By contrast, in most ARCI patients, these genes carry missense mutations, and thus, their protein products retain some residual activity. In this situation, the ceramide composition of the SC of these patients may not necessarily be consistent with that predicted by studies of the corresponding gene-knockout mice. Furthermore, the ceramide composition of the SC differs greatly between humans and mice.[9] For example, humans have many H-, P-, and A-type ceramides, whereas mice have no H-type ceramides and fewer P- and A-type ceramides than humans. Instead, mouse SC contains more O-type ceramides and abundant β-hydroxy (B)-type ceramides, which contain β-hydroxy FAs and are absent in humans. Here, we

comprehensively analyzed the ceramides in the SC of an ARCI patient with residual CERS3 activity. We obtained an unexpected result: the levels of protein-bound ceramides were normal, whereas those of acylceramides were greatly reduced (Figs. 4 and 5). These results indicate for the first time that a decrease in the levels of acylceramides alone causes ichthyosis.

A lack of correlation between the levels of acylceramides and protein-bound ceramides was also observed in mice in which the gene encoding the acyl-CoA synthetase *Fatp4* had been knocked out.[32] In the acylceramide synthesis pathway, FATP4 catalyzes the conversion of ω-hydroxy FAs to ω-hydroxy acyl-CoAs, which act as CERS3 substrates.[32] Acylceramide levels in the *Fatp4* knockout mice were reduced to approximately one-tenth of those in WT mice, but protein-bound ceramides were only reduced to approximately two-thirds of the WT levels.

In this study, we observed no correlation between the levels of acylceramides and protein-bound ceramides in an ichthyosis patient with *CERS3* mutations, possibly because of a change in the arrangement of the acylceramides within the lipid lamellae. Under normal conditions, most acylceramides are regularly arranged within the lipid lamellae and spatially separated from the CLE region. Only those few acylceramides that are adjacent to the corneocyte cell surface may be converted to protein-bound ceramides to form the CLE. By contrast, when acylceramide levels are reduced (as in the patient in this study), the lamellar structure is disturbed, allowing acylceramides to diffuse more freely. Consequently, acylceramides may become accessible to the corneocyte cell surface and converted to protein-bound ceramides until the corneocytes are fully covered with protein-bound ceramides. As a result, while normal quantities of protein-bound ceramides are produced, acylceramide levels are reduced. Another possibility is that reduced acylceramide synthesis indirectly causes the expression of the genes involved in the synthesis of protein-bound ceramides to increase. Indeed, *ALOX12B* and

ALOXE3 mRNA levels have been reported to increase to 232% and 149% of normal levels, respectively, in cultured keratinocytes from ichthyosis patients with homozygous p.Trp15Arg mutations in *CERS3*.[13]

The patient in this study exhibited increases in the total levels of NS and AS classes and a decrease in acylceramide levels (Fig. 4). The increases were mainly due to increases in species containing C14–C24 FAs (Fig. 4, Supplementary Table S2). The FA composition of ceramides/sphingolipids in each tissue is mainly determined by the balance of the expression levels of CERS isozymes, each of which exhibits its own substrate specificity (CERS1, C18; CERS2, C22–C24; CERS3, ≥ C26; CERS4, C22; and CERS5 and CERS6, C16).[6] For example, C24 ceramides/sphingolipids are abundant in the liver and kidney, where *CERS2* expression is high, and C18 ceramides/sphingolipids are abundant in neurons, in which *CERS1* expression is high.[33,34] Overexpression of any one CERS isozyme results in an increase in the proportion of ceramides with the chain lengths that isozyme exhibits the highest levels of activity toward, and in a decrease in the proportion of those with other chain lengths.[35] Knockout or knockdown of that isozyme has the opposite effect.[36,37] The *CERS3* mutations may thus cause FA shortening in all ceramide species. FAs with a chain length of ≤ C26 cannot become acylceramides, since FA ω-hydroxylase (human CYP4F22, mouse Cyp4f39), which acts in the acylceramide synthesis pathway, exhibits high levels of activity toward ≥ C28 FAs only.[20] Therefore, FA shortening in ceramides would lead to a shift in the balance of ceramide species away from acylceramides toward non-acylated ceramides (e.g., NS, AS, and NDS; Fig. 4).

In this study, we investigated in detail the SC ceramide composition of an ichthyosis patient who exhibited a significant reduction in, but not complete abrogation of, CERS3 activity. In this patient, we observed altered ceramide composition, including reduced acylceramide levels,

although the levels of protein-bound ceramides were almost unchanged. However, ichthyosis patients with other *CERS3* mutations may exhibit different ceramide composition and symptom severity from the patient in this study, due to differences in the strength of the effects on enzyme activity. It is therefore important to investigate the SC ceramide composition of patients with *CERS3* mutations as well as patients with mutations in other ceramide-related genes, in order to understand the pathogenesis of ichthyosis.

ACKNOWLEDGMENTS

This work was supported by the Lydia O'Leary Memorial Pias Dermatological Foundation, by the Advanced Research and Development Programs for Medical Innovation (AMED-CREST) (Grant Number JP20gm0910002h0006 to AK) from the Japan Agency for Medical Research and Development (AMED), and by KAKENHI (Grant Number JP18H03976 to AK) from the Japan Society for the Promotion of Science.

CONFLICT OF INTEREST

None declared.

REFERENCES

1 Goleva E, Berdyshev E, Leung DY. Epithelial barrier repair and prevention of allergy. *J Clin Invest* 2019; **129**: 1463-74.

2 Takeichi T, Akiyama M. Inherited ichthyosis: Non-syndromic forms. *J Dermatol* 2016; **43**: 242-51.

3 Vahlquist A, Fischer J, Törmä H. Inherited Nonsyndromic Ichthyoses: An Update on Pathophysiology, Diagnosis and Treatment. *Am J Clin Dermatol* 2018; **19**: 51-66.

4 Feingold KR, Elias PM. Role of lipids in the formation and maintenance of the cutaneous permeability barrier. *Biochim Biophys Acta* 2014; **1841**: 280-94.

5 Breiden B, Sandhoff K. The role of sphingolipid metabolism in cutaneous permeability barrier formation. *Biochim Biophys Acta* 2014; **1841**: 441-52.

6 Kihara A. Synthesis and degradation pathways, functions, and pathology of ceramides and epidermal acylceramides. *Prog Lipid Res* 2016; **63**: 50-69.

7 Elias PM, Gruber R, Crumrine D *et al.* Formation and functions of the corneocyte lipid envelope (CLE). *Biochim Biophys Acta* 2014; **1841**: 314-8.

8 Muñoz-Garcia A, Thomas CP, Keeney DS *et al*. The importance of the lipoxygenase-hepoxilin pathway in the mammalian epidermal barrier. *Biochim Biophys Acta* 2014; **1841**: 401-8.

9 Kawana M, Miyamoto M, Ohno Y *et al.* Comparative profiling and comprehensive quantification of stratum corneum ceramides in humans and mice by LC/MS/MS. *J Lipid Res* 2020; **61**: 884-95.

10 Takeichi T, Hirabayashi T, Miyasaka Y *et al.* SDR9C7 catalyzes critical dehydrogenation of acylceramides for skin barrier formation. *J Clin Invest* 2020; **130**: 890-903.

11 Jennemann R, Rabionet M, Gorgas K *et al.* Loss of ceramide synthase 3 causes lethal skin barrier disruption. *Hum Mol Genet* 2012; **21**: 586-608.

12 Radner FP, Marrakchi S, Kirchmeier P *et al.* Mutations in CERS3 cause autosomal recessive congenital ichthyosis in humans. *PLoS Genet* 2013; **9**: e1003536.

13 Eckl KM, Tidhar R, Thiele H *et al.* Impaired epidermal ceramide synthesis causes autosomal recessive congenital ichthyosis and reveals the importance of ceramide acyl chain length. *J Invest Dermatol* 2013; **133**: 2202-11.

14 Polubothu S, Glover M, Holder SE *et al.* Uniparental disomy as a mechanism for CERS3-mutated autosomal recessive congenital ichthyosis. *Br J Dermatol* 2018; **179**: 1214-15.

15 Youssefian L, Vahidnezhad H, Saeidian AH *et al.* Autosomal recessive congenital ichthyosis: CERS3 mutations identified by a next generation sequencing panel targeting ichthyosis genes. *Eur J Hum Genet* 2017; **25**: 1282-85.

16 Youssefian L, Vahidnezhad H, Saeidian AH *et al.* Autosomal recessive congenital ichthyosis: Genomic landscape and phenotypic spectrum in a cohort of 125 consanguineous families. *Hum Mutat* 2019; **40**: 288-98.

17 Jojima K, Edagawa M, Sawai M *et al.* Biosynthesis of the anti-lipid-microdomain sphingoid base 4,14-sphingadiene by the ceramide desaturase FADS3. *FASEB J* 2020; **34**: 3318-35.

18 Kihara A, Anada Y, Igarashi Y. Mouse sphingosine kinase isoforms SPHK1a and SPHK1b differ in enzymatic traits including stability, localization, modification, and oligomerization. *J Biol Chem* 2006; **281**: 4532-9.

19 Sassa T, Ohno Y, Suzuki S *et al.* Impaired epidermal permeability barrier in mice lacking elovl1, the gene responsible for very-long-chain fatty acid production. *Mol Cell Biol* 2013; **33**: 2787-96.

20 Ohno Y, Nakamichi S, Ohkuni A *et al.* Essential role of the cytochrome P450 CYP4F22 in the production of acylceramide, the key lipid for skin permeability barrier formation. *Proc Natl Acad Sci U S A* 2015; **112**: 7707-12.

21 Kitamura T, Takagi S, Naganuma T *et al.* Mouse aldehyde dehydrogenase ALDH3B2 is localized to lipid droplets via two C-terminal tryptophan residues and lipid modification. *Biochem J* 2015; **465**: 79-87.

22 Mizutani Y, Kihara A, Igarashi Y. Mammalian Lass6 and its related family members regulate synthesis of specific ceramides. *Biochem J* 2005; **390**: 263-71.

23 Spassieva S, Seo JG, Jiang JC *et al.* Necessary role for the Lag1p motif in (dihydro)ceramide synthase activity. *J Biol Chem* 2006; **281**: 33931-8.

24 Kihara A. Very long-chain fatty acids: elongation, physiology and related disorders. *J Biochem* 2012; **152**: 387-95.

25 Sassa T, Kihara A. Metabolism of very long-chain Fatty acids: genes and pathophysiology. *Biomol Ther (Seoul)* 2014; **22**: 83-92.

26 Wertz PW, Madison KC, Downing DT. Covalently bound lipids of human stratum corneum. *J Invest Dermatol* 1989; **92**: 109-11.

27 Grond S, Eichmann TO, Dubrac S *et al.* PNPLA1 deficiency in mice and humans leads to a defect in the synthesis of omega-O-acylceramides. *J Invest Dermatol* 2017; **137**: 394-402.

28 Hirabayashi T, Anjo T, Kaneko A *et al.* PNPLA1 has a crucial role in skin barrier function by directing acylceramide biosynthesis. *Nat Commun* 2017; **8**: 14609.

29 Miyamoto M, Itoh N, Sawai M *et al.* Severe skin permeability barrier dysfunction in knockout mice deficient in a fatty acid ω-hydroxylase crucial to acylceramide production. *J Invest Dermatol* 2020; **140**: 319-26.e4.

30 Epp N, Fürstenberger G, Müller K *et al.* 12R-lipoxygenase deficiency disrupts epidermal barrier function. *J Cell Biol* 2007; **177**: 173-82.

31 Krieg P, Rosenberger S, de Juanes S *et al. Aloxe3* knockout mice reveal a function of epidermal lipoxygenase-3 as hepoxilin synthase and its pivotal role in barrier formation. *J Invest Dermatol* 2013; **133**: 172-80.

32 Yamamoto H, Hattori M, Chamulitrat W *et al.* Skin permeability barrier formation by the ichthyosis-causative gene *FATP4* through formation of the barrier lipid ω-*O*-acylceramide. *Proc Natl Acad Sci U S A* 2020; **117**: 2914-22.

33 Imgrund S, Hartmann D, Farwanah H *et al.* Adult ceramide synthase 2 (CERS2)-deficient mice exhibit myelin sheath defects, cerebellar degeneration, and hepatocarcinomas. *J Biol Chem* 2009; **284**: 33549-60.

34 Zhao L, Spassieva SD, Jucius TJ *et al.* A deficiency of ceramide biosynthesis causes cerebellar purkinje cell neurodegeneration and lipofuscin accumulation. *PLoS Genet* 2011; **7**: e1002063.

35 Sassa T, Hirayama T, Kihara A. Enzyme activities of the ceramide synthases CERS2-6 are regulated by phosphorylation in the C-terminal region. *J Biol Chem* 2016; **291**: 7477-87.

36 Park JW, Park WJ, Futerman AH. Ceramide synthases as potential targets for therapeutic intervention in human diseases. *Biochim Biophys Acta* 2014; **1841**: 671-81.

37 Sassa T, Suto S, Okayasu Y *et al.* A shift in sphingolipid composition from C24 to C16 increases susceptibility to apoptosis in HeLa cells. *Biochim Biophys Acta* 2012; **1821**: 1031-7.

SUPPORTING INFORMATION

Additional Supporting Information may be found in the online version of this article:

Figure S1. Compound heterozygous *CERS3* mutations. (a, b) Assembly of the sequence reads covering the region with the g.101031087G>A mutation (a) or the g.101013181C>T mutation (b) obtained by whole-exome sequencing of the patient's genomic DNA.

Table S1. Quantities and proportions of ceramide classes.

Table S2. Quantities of ceramide species.

Table S3. Quantities and proportions of each protein-bound ceramide class.

Table S4. Quantities of protein-bound ceramide species.

FIGURE LEGENDS

Figure 1. Structures and nomenclature of human ceramide classes. (a) Structure of a ceramide and an acylceramide. The ceramide synthase CERS3 catalyzes amide bond formation between a long-chain base (LCB) and a fatty acid (FA) with ≥ C26. (b) Structures of human LCBs. (c) Structures of FAs constituting human ceramides. The chain lengths of N- and A-type FAs are mainly C16–C28 (n = 1–13 in the figure), whereas those of O-, EO-, and P-O-type FAs are C28–C36 (n = 11–19 in the figure). (d) Nomenclature of 25 ceramide classes comprising 20 classes of free ceramides and five of protein-bound ceramides. Each ceramide class is represented by a combination of the abbreviations corresponding to its FA and LCB moieties.

Figure 2. Clinical features of the patient and positions of the mutations. (a) Patient at two months of age. Erythroderma with fine scale, wrinkles, and limited desquamation can be seen. (b) Pedigree tree of the ichthyosis patient with *CERS3* mutations and the DNA sequences of the patient and his parents, obtained via Sanger sequencing. (c) Positions of the mutations in the predicted CERS3 membrane topology, and changes in amino acid residues, in the patient. ER, endoplasmic reticulum.

Figure 3. Reduced ceramide synthase activity of CERS3 mutants. HEK 293T cells were transfected with the plasmid encoding *3×FLAG-CERS3* wild-type (WT), p.Arg75*, or p.Arg229His, together with the plasmid encoding *3×FLAG-ELOVL1*. (a) Transfected cells were incubated with 5 μM seven deuterium (d_7) atom-containing dihydrosphingosine for 3 h, after which lipids were extracted from the cells. Levels of d_7-C26:0 NS ceramide were measured via liquid chromatography–tandem mass spectrometry. Values presented are the

means ± standard deviations of three independent experiments. Statistically significant differences are indicated: $^{**}P < 0.01$ (Tukey's test). (b) Total cell lysates (5 μg) prepared from the transfected cells were subjected to immunoblotting using anti-FLAG antibody.

Figure 4. Ceramide profile change in the patient's stratum corneum. Stratum corneum samples were collected from the patient and three healthy controls. From each tape strip, three pieces were cut, and each piece was subjected to lipid extraction and ceramide measurement through liquid chromatography–tandem mass spectrometry. The mean of the measurement results from the three pieces was used as the value for each person. Values represent means (three healthy controls) ± standard deviations or means (one patient). (a) Total quantity of each ceramide class. (b) Ratio of each ceramide class to total ceramides. (c, d) Proportions of ceramide classes containing the indicated long-chain base type (c) or fatty acid type (d). (e–g) Fatty acid composition of (e) NS, (f) AS, and (g) EOS classes. n.d., not detected.

Figure 5. Normal levels of protein-bound ceramides in the patient's stratum corneum. Stratum corneum samples were collected from the patient and three healthy controls. From each tape strip, three pieces were cut, and each piece was subjected to lipid extraction and protein-bound ceramide measurement through liquid chromatography–tandem mass spectrometry. The mean of the measurement results obtained from the three pieces is used as the value for each person. Values represent means (means of three healthy controls) ± standard deviations or means (one patient). (a) Total quantity of each protein-bound ceramide class. Values are the sum of the protein-bound ceramide species containing each fatty acid chain length. (b) Fatty acid composition of P-OS. n.d., not detected.

Figure 1

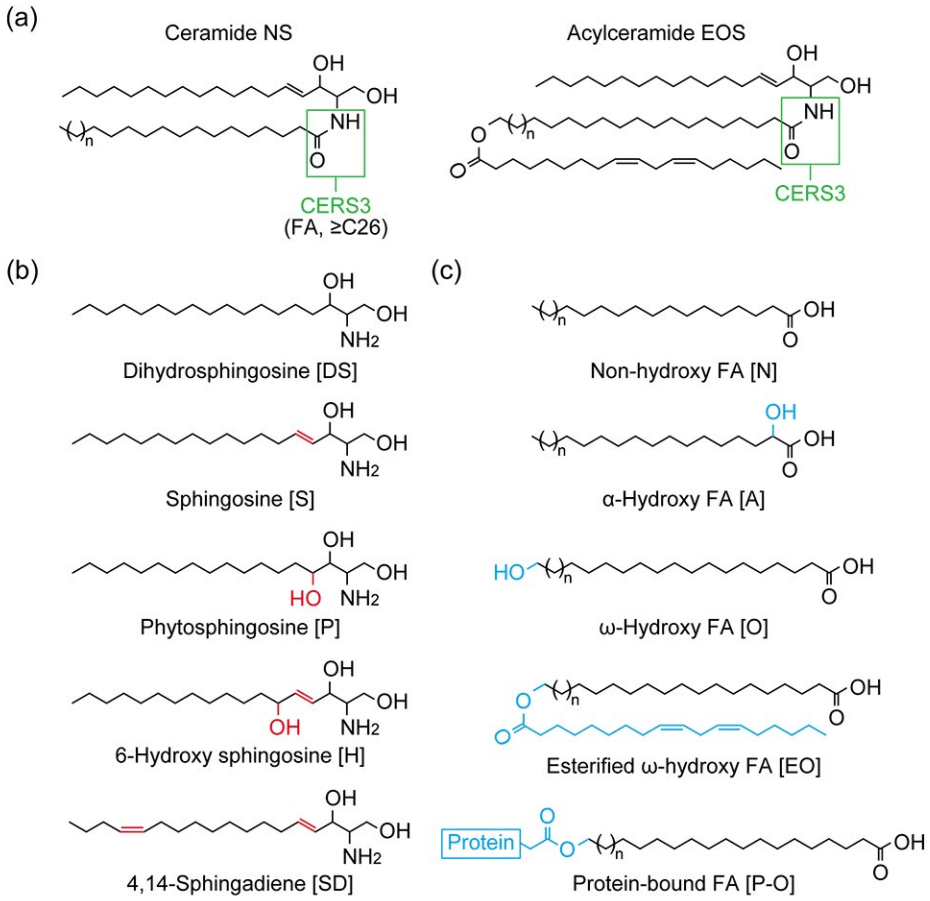

(d)

LCBs \ FAs	Non-hydroxy [N]	α-Hydroxy [A]	ω-Hydroxy [O]	Esterified ω-hydroxy [EO]	Protein-bound ω-hydroxy [P-O]
Dihydrosphingosine [DS]	**NDS**	**ADS**	**ODS**	**EODS**	**P-ODS**
Sphingosine [S]	**NS**	**AS**	**OS**	**EOS**	**P-OS**
Phytosphingosine [P]	**NP**	**AP**	**OP**	**EOP**	**P-OP**
6-Hydroxy sphingosine [H]	**NH**	**AH**	**OH**	**EOH**	**P-OH**
4,14-Sphingadiene [SD]	**NSD**	**ASD**	**OSD**	**EOSD**	**P-OSD**

Acylceramides
Protein-bound ceramides

Figure 2

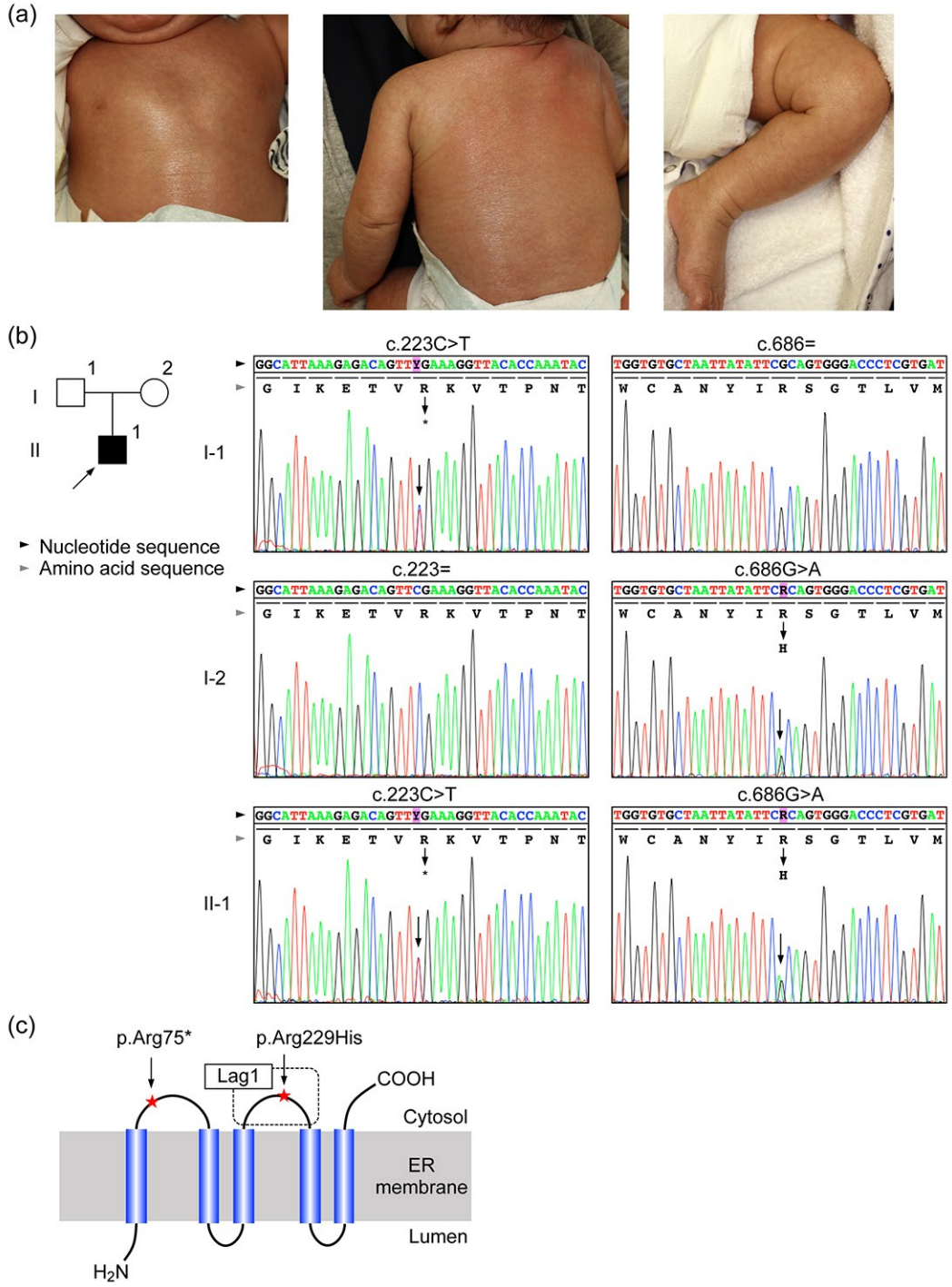
(a)
(b)
I
II
1
2
1
Nucleotide sequence
Amino acid sequence
c.223C>T
c.686=
I-1
c.223=
c.686G>A
I-2
c.223C>T
c.686G>A
II-1
(c)
p.Arg75*
p.Arg229His
Lag1
COOH
Cytosol
ER membrane
Lumen
H2N

Figure 3

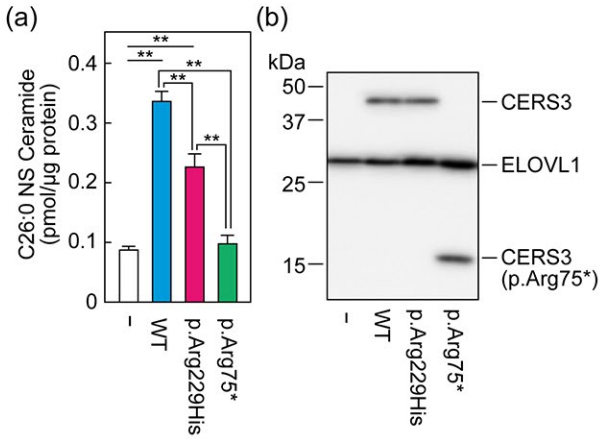
(a)
(b)
C26:0 NS Ceramide (pmol/μg protein)
0.4
0.3
0.2
0.1
0
**
**
**
**
**
–
WT
p.Arg229His
p.Arg75*
kDa
50
37
25
15
CERS3
ELOVL1
CERS3 (p.Arg75*)
–
WT
p.Arg229His
p.Arg75*

Figure 4

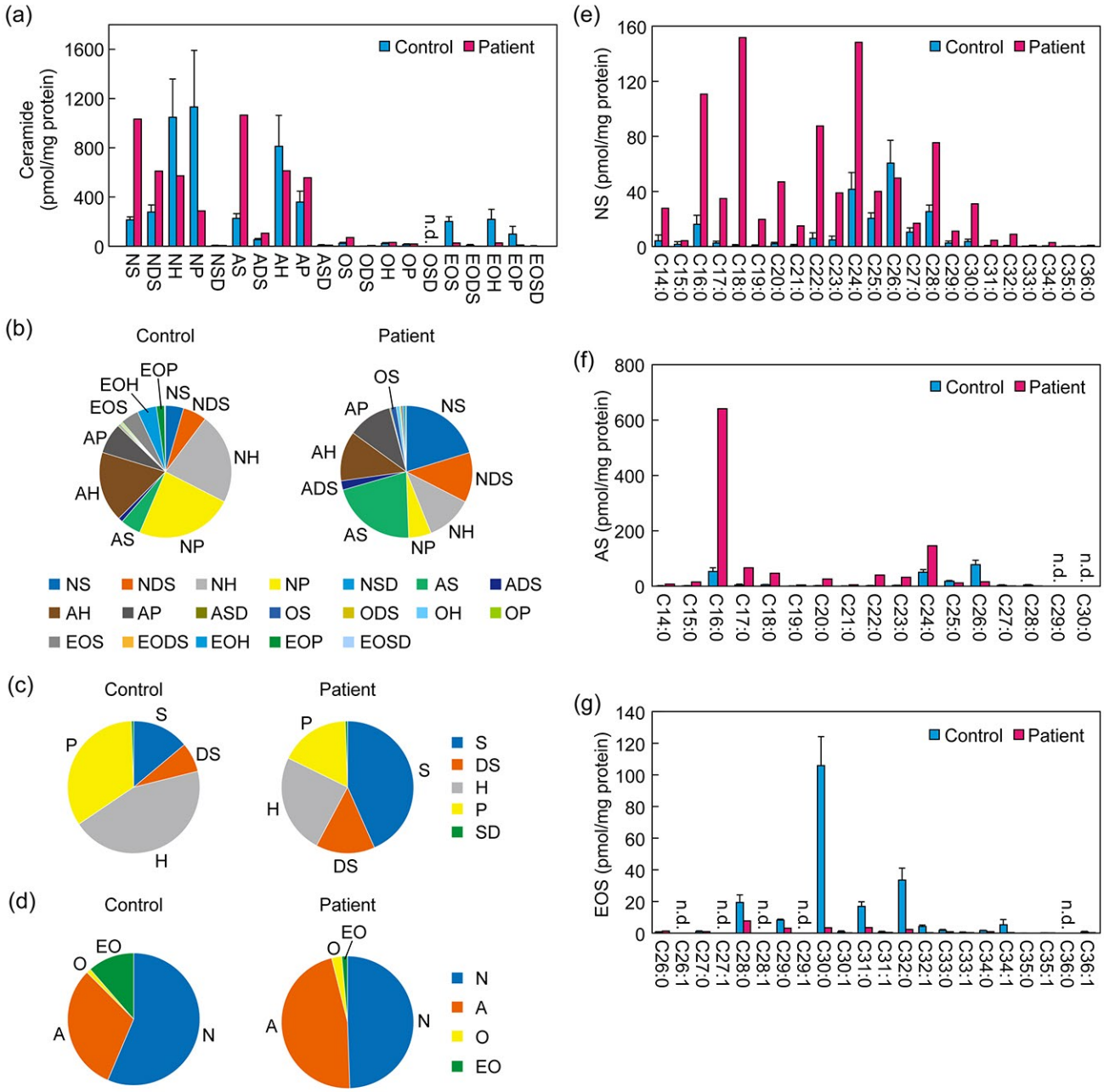
(a)
Ceramide (pmol/mg protein)
Control
Patient
NS NDS NH NP NSD AS ADS AH AP ASD OS ODS OH OP OSD EOS EODS EOH EOP EOSD
n.d.
(b)
Control
Patient
NS NDS NH NP NSD AS ADS AH AP ASD OS ODS OH OP EOS EODS EOH EOP EOSD
(c)
Control
Patient
S DS H P SD
(d)
Control
Patient
N A O EO
(e)
NS (pmol/mg protein)
Control
Patient
(f)
AS (pmol/mg protein)
Control
Patient
n.d.
(g)
EOS (pmol/mg protein)
Control
Patient
n.d.

Figure 5

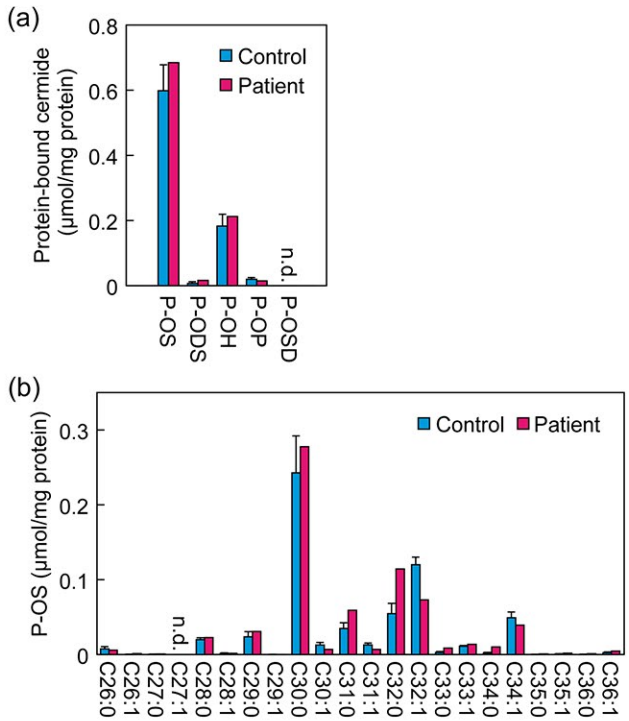
(a)
Protein-bound cermide (μmol/mg protein)
0.8
0.6
0.4
0.2
0
Control
Patient
n.d.
P-OS
P-ODS
P-OH
P-OP
P-OSD
(b)
P-OS (μmol/mg protein)
0.3
0.2
0.1
0
Control
Patient
n.d.
C26:0
C26:1
C27:0
C27:1
C28:0
C28:1
C29:0
C29:1
C30:0
C30:1
C31:0
C31:1
C32:0
C32:1
C33:0
C33:1
C34:0
C34:1
C35:0
C35:1
C36:0
C36:1